Molecular Vision 2014; 20:1146-1159 <http://www.molvis.org/molvis/v20/1146>
Received 23 January 2012 | Accepted 1 August 2014 | Published 4 August 2014

Role of *FAM18B* in diabetic retinopathy

Ai Ling Wang,[1] Vidhya R. Rao,[1] Judy J. Chen,[1] Yves A. Lussier,[2] Jalees Rehman,[3] Yong Huang,[4] Rama D. Jager,[5] Michael A. Grassi[1]

(The first two authors contributed equally to this work.)

[1]Department of Ophthalmology and Visual Sciences, University of Illinois at Chicago, Chicago, IL; [2]Department of Medicine, University of Arizona, Tucson, AZ; [3]Departments of Medicine and Pharmacology, University of Illinois at Chicago, Chicago, IL; [4]Section of Gastroenterology, Department of Medicine, University of Chicago, Chicago, IL; [5]University Retina, Oak Forest, IL

Purpose: Genome-wide association studies have suggested an association between a previously uncharacterized gene, *FAM18B*, and diabetic retinopathy. This study explores the role of *FAM18B* in diabetic retinopathy. An improved understanding of *FAM18B* could yield important insights into the pathogenesis of this sight-threatening complication of diabetes mellitus.

Methods: Postmortem human eyes were examined with immunohistochemistry and immunofluorescence for the presence of *FAM18B*. Expression of FAM18B in primary human retinal microvascular endothelial cells (HRMECs) exposed to hyperglycemia, vascular endothelial growth factor (VEGF), or advanced glycation end products (AGEs) was determined with quantitative reverse-transcription PCR (qRT-PCR) and/or western blot. The role of *FAM18B* in regulating human retinal microvascular endothelial cell viability, migration, and endothelial tube formation was determined following RNAi-mediated knockdown of *FAM18B*. The presence of *FAM18B* was determined with qRT-PCR in CD34+/VEGFR2+ mononuclear cells isolated from a cohort of 17 diabetic subjects with and without diabetic retinopathy.

Results: Immunohistochemistry and immunofluorescence demonstrated the presence of *FAM18B* in the human retina with prominent vascular staining. Hyperglycemia, VEGF, and AGEs downregulated the expression of *FAM18B* in HRMECs. RNAi-mediated knockdown of *FAM18B* in HRMECs contributed to enhanced migration and tube formation as well as exacerbating the hyperglycemia-induced decrease in HRMEC viability. The enhanced migration, tube formation, and decrease in the viability of HRMECs as a result of *FAM18B* downregulation was reversed with pyrrolidine dithiocarbamate (PDTC), a specific nuclear factor-kappa B (NF-κB) inhibitor. CD34+/VEGFR2+ mononuclear cells from subjects with proliferative diabetic retinopathy demonstrated significantly reduced mRNA expression of *FAM18B* compared to diabetic subjects without retinopathy.

Conclusions: *FAM18B* is expressed in the retina. Diabetic culture conditions decrease the expression of FAM18B in HRMECs. The downregulation of *FAM18B* by siRNA in HRMECs results in enhanced migration and tube formation, but also exacerbates the hyperglycemia-induced decrease in HRMEC viability. The pathogenic changes observed in HRMECs as a result of *FAM18B* downregulation were reversed with PDTC, a specific NF-κB inhibitor. This study is the first to demonstrate a potential role for *FAM18B* in the pathogenesis of diabetic retinopathy.

Diabetic retinopathy is currently the leading cause of irreversible vision loss in working-age adults in the United States [1]. Diabetic retinopathy is a complex disease that affects the normal functioning of retinal vasculature, neurons, and resident glial cells. Several factors including hyperglycemia, advanced glycation end products (AGEs), and cytokines such as vascular endothelial growth factor (VEGF) have been implicated in the disease pathogenesis [2]. Hyperglycemia contributes to endothelial cell dysfunction, endothelial cell death by apoptosis, and ultimately the loss of retinal capillary microvasculature observed in diabetic retinopathy [3,4]. VEGF has been implicated as a key mediator in enhancing vascular permeability and endothelial cell survival, proliferation, migration, and neovascularization in advanced stages of diabetic retinopathy [5-7]. The pathogenic effects of high glucose and VEGF in endothelial cells have been attributed in part to enhanced activation of proinflammatory transcription factor nuclear factor-kappa B (NF-κB) [8-11]. Current preventive measures including glycemic control are beneficial in delaying the progression of the disease; however, they have had limited success in treating advanced stages of the disease. Although early detection and effective preventive measures are of major significance for preventing diabetic retinopathy, there is also a need to identify additional pathogenic mechanisms in the retinal vasculature that might serve as putative therapeutic targets.

Correspondence to: Michael A. Grassi, Retina Chemical Genomics Laboratory, Lions of Illinois Eye Research Institute, University of Illinois at Chicago, 1855 W. Taylor St., M/C 648, Chicago, IL, 60612-7244; Phone: (312) 413-7347; FAX: (312) 996-7773; email: grassim@uic.edu

Dr. Wang is now at Department of Ophthalmology and Visual Sciences, Albert Einstein College of Medicine of Yeshiva University, Bronx, NY.

Although glycemic control and diabetes duration are important predictors of retinopathy [1,12], genetic susceptibility also plays an important role in the pathogenesis of diabetic retinopathy [13]. Identification and characterization of genetic factors that predispose individuals to diabetic retinopathy could improve prevention and treatment measures for this debilitating condition. In the search for genetic elements that underlie diabetic retinopathy, we previously performed a genome-wide association study (GWAS) [14,15]. An interesting finding generated from the analysis is the association of diabetic retinopathy with an SNP, rs11871508, in encoding family with sequence similarity 18, member B (*FAM18B;* gene ID 51030) also known as trans-Golgi network vesicle protein 23 homolog B (TVP23B). *FAM18B* is located on chromosome 17 [16]. The function of *FAM18B* is unknown. However, the protein encoded is expected to be an integral membrane protein. Given its association with diabetic retinopathy in our study, we sought to explore the possible role of *FAM18B* in diabetic retinopathy. Herein, we find that *FAM18B* is expressed in diabetic retinopathy–relevant tissues. We also demonstrate functional changes in human retinal microvascular endothelial cells with RNAi-induced downregulation of *FAM18B*. Overall, this study supports a role of *FAM18B* in the pathogenesis of diabetic retinopathy.

METHODS

Institutional review board approval: The samples were obtained from all subjects through an approved institutional review board (IRB) protocol at the consenting institution. The use of human blood samples was approved by the University of Illinois, Chicago Institutional Review Board, and all participants gave informed consent to participate in the study. Since all patient health information was de-identified before genotyping and analysis, the IRB at the University of Illinois, Chicago, declared this portion of the study to be non-human subjects research.

Human subjects: Use of all human tissue conformed to the Declaration of Helsinki and the policies of the University of Illinois at Chicago. The subject characteristics are described in Table 1. All participants underwent a complete medical history, and all subjects received an ophthalmic clinical evaluation. Participants included a study group consisting of subjects with proliferative diabetic retinopathy (PDR; n=8) and age-matched subjects with diabetes but without diabetic retinopathy (n=9; Table 1). The clinical diagnosis of proliferative diabetic retinopathy was defined as active neovascularization visible on the retina, tractional retinal detachment from fibrosis, or a diabetic vitreous hemorrhage in at least one eye. Age-matched diabetic controls were identified by an ophthalmologist as having no background diabetic retinopathy at the time of sample collection as well as no history of active neovascularization or diabetic macular edema.

Adult peripheral blood samples: Human peripheral blood samples were obtained from the subjects by venipuncture and collected in sodium heparin tubes (Vacutainer CPT; BD Labware, Bedford, MA). The tubes were prepared with a FICOLL Hypaque density fluid, allowing for separation of mononuclear precursor cells in a single step. Isolated mononuclear precursor cells were collected, washed twice, and resuspended in PBS (pH 7.4; Cat No# 14190250. Life Technologies, Carlsbad, CA).

Donor eyes: Eyes from two post-mortem donors were used in this study. The retinal sections of the left eye of normal human donors were used in the study. The retinal sections of the human donors were obtained from the Illinois Eye Bank (Chicago, IL). Post-mortem donor eyes were supplied by Midwest Eye Bank (Ann Arbor, MI).

Table 1. Demographic and baseline characteristics of subjects (n = 17).

Characteristics	Control (n=9) (DM w/o PDR)	Experimental (n=8) (DM w/ active PDR)	P value (t test)
Age at collection, mean (SD), in years	56.8 (14.6)	59.1 (12.4)	0.73
	Gender		
Male, n (% of total)	6 (66.7)	3 (37.5)	0.26
Female, n (% of total)	3 (33.3)	5 (62.5)	
	Race/Ethnicity		
Caucasian, n (% of total)	1 (11.1)	1 (12.5)	0.62
African American, n (% of total)	8 (88.9)	7 (75.0)	
Hispanic, n (% of total)	0 (0.00)	1 (12.5)	
Diabetes duration, mean (SD), years	9.9 (6.5)	18.3 (12.6)	0.22
BSL at last visit, mean (SD), mg/dl	143.4 (36.7)	195.6 (54.6)	0.06

Cell culture: Primary human retinal microvascular endothelial cells (HRMECs, ACBRI 181, Cell Systems, Kirkland, WA) were maintained in MCDB 131 medium containing 10% fetal calf serum (FCS, Invitrogen, Life Technologies, Carlsbad, CA), 100 IU/ ml penicillin, 100 µg/ml streptomycin, and 0.25 µg/ml amphotericin B supplemented with 1 µg/ml epidermal growth factor and 10 µg/ml hydrocortisone (complete medium). The cell surface was coated with gelatin-based coating solution to provide optimum growth surface. All experiments using HRMECs were performed between passages 5 and 8. The cells were serum starved for 24 h for all experiments unless mentioned otherwise. For mRNA expression, HRMECs were grown to confluence in 24-well plates. Following serum starvation, the cells were treated with media containing normal glucose (5 mM), high glucose (25 mM), VEGF (1 ng/ml; Recombinant human VEGF 165, R&D systems, Minneapolis, MN), and AGEs (Sigma A8301) for 24 h. For the protein expression studies, HRMECs were grown to confluence in six-well plates. Following serum starvation, the cells were treated with serum and growth factor-free media (medium alone) containing normal glucose (5 mM), high glucose (30 mM), or VEGF (50 ng/ml) for 48 h. For RNAi-mediated downregulation of *FAM18B*, the cells were seeded at a density of 200,000 cells/well in six-well plates or 20,000 cells/well in 96-well plates in complete medium. Cells were reverse transfected for 72 h with negative control siRNA (Silencer Select, Cat# 4,390,846, Life Technologies) and *FAM18B* siRNA (Silencer Select, Cat# 4,392,420, Life Technologies) at a final concentration of 50 nM using the Lipofectamine RNAiMAX Transfection Reagent (Life Technologies) according to the manufacturer's instructions.

Immunohistochemistry and Immunofluorescence: Donor eyes were fixed in 10% buffered formaldehyde, washed in PBS (pH 7.4), embedded in paraffin, and sectioned. The tissue sections were treated with xylene and a series of graded ethanol steps and rehydrated in PBS. The tissues were heated at 95 °C to 99 °C in citrate buffer (pH 6.0) for 20 min for antigen retrieval. The sections were blocked with 5% normal goat serum for 20 min and incubated at 4 °C overnight with the rabbit polyclonal anti-*FAM18B* primary antibody (1:100, Sigma-Aldrich, St. Louis, MO, HPA019585). Primary antibody was omitted in the negative control. For immunohistochemistry, the Vectastain Elite ABC kit (Vector Laboratories, Burlingame, CA) was used with diaminobenzidine as a substrate. As a negative control, sections were treated in the same manner, except that incubation with primary antibody was omitted. The sections were treated for equal time in 3,3′-diaminobenzidine and photographed with the antibody-containing tissue. For immunofluorescence, the tissue sections were incubated with 1:1,000 secondary antibody, Alexa Fluor 594 goat anti-rabbit immunoglobulin G (IgG; Molecular Probes, Eugene, OR) for 1 h at room temperature. After washing with PBS, the slides were mounted with Vectashield containing 4',6-diamidino-2-phenylindole (DAPI; Vector Laboratories) and observed using confocal microscopy.

Quantitative real-time quantitative polymerase chain reaction: Total cellular RNA was isolated and purified (PicoPure; Arcturus, Mountain View, CA). Samples of the total starting RNA were analyzed with capillary electrophoresis (Agilent Technologies, Palo Alto, CA) to assess the degree of purification. RNAs with RIN less than 8.9 were not used in the study. Real-time quantitative reverse-transcription–PCR (qRT-PCR) was performed using the SYBR Green dye binding method implemented on an Applied Biosystems 7900 genetic analyzer (Applied Biosystems, Foster City, CA) at the DNA Services Facility at the University of Illinois at Chicago. 2.0 µl cDNA samples were amplified with specific primers for FAM18B (5'-TGT TTG ATG CGG AAG AGG AGA CGA-3' ; 5'- AAT AAA GCT GCT GCT GAG CAA CCC-3') and GAPDH (5'-ACA TCG CTC AGA CAC CAT G-3'; 3'-TGT AGT TGA GGT CAA TGA AGG G-5') using power SYBR Green PCR master mix (Life Technologies). qPCR amplifications were performed for 40 cycles of denaturation at 95 °C for 15 s, annealing/extension 60 °C for 60 s as described by the manufacturer's instructions. The amplifications The melting curves were generated to detect the melting temperatures of the specific products immediately after the PCR run. Validated primers for each gene of interest were designed for each target mRNA. To ensure appropriate cycle time response, the primers were optimized, and the input cDNA levels were determined. Relative expression was calculated from the differences in the cycle time of an internal standard (glyceraldehyde 3-phosphate dehydrogenase; GAPDH) compared to the target mRNA. All qRT-PCR reactions used 40 ng of cDNA produced as described above and were run with two sets of triplicates.

Western blot analysis: Following the treatments, the HRMECs were rinsed with cold PBS. The cells were collected in 1 ml PBS, collected in a microcentrifuge tube, and pelleted at 300 ×*g* for 10 min. The PBS was discarded, and the cells were lysed in 150 µl of lysis buffer (ProteoJET mammalian cell lysis reagent, Fermentas Life Sciences, Pittsburgh, PA) containing protease inhibitors (Roche, Diagnostics, Indianapolis, IN). Following lysis on ice for 20 min, the lysates were clarified with centrifugation at 300 ×*g* for 10 min. The protein content was estimated using the bicinchoninic acid (BCA) kit (Pierce Biotechnology, Rockford, IL). Lysates with equal amounts of protein were supplemented with sodium dodecyl sulfate (SDS) sample buffer and resolved with 10%

SDS–polyacrylamide gel electrophoresis (PAGE). Resolved proteins were transferred to 0.2 µ nitrocellulose membrane (Cell Signaling Technology, Beverly, MA) overnight at 4 °C. The membranes were blocked with 5% bovine serum albumin (BSA) in TBS/T (10 mM Tris pH 7.4, 140 mM NaCl, 0.1% (V/V) Tween 20) for 1 h at room temperature and probed with 1:100 dilution of primary anti-human rabbit polyclonal *FAM18B* antibody (1:100, Sigma-Aldrich, HPA019585) at 4 °C overnight. Following washes in TBS/T, the membranes were incubated with 1:3,000 anti-rabbit horseradish peroxidase (HRP) conjugated secondary antibody (Bio-Rad, Des Plaines, IL). The blots were developed with the Super Signal West Pico Substrate kit (Pierce Biotechnology). The blots were stripped and reprobed with 1:1,000 dilution of anti-human mouse monoclonal anti beta-tubulin antibody (Sigma-Aldrich, T8328) followed by 1:3,000 anti-mouse HRP conjugated secondary antibody (Bio-Rad) to normalize protein loading. The blots were developed using SuperSignal West Pico chemiluminescent substrate (Thermo Scientific, Rockford, IL). Densitometric analysis of the bands was performed using the image-analysis software (ImageJ; National Institutes of Health, Bethesda, MD).

Flow cytometry and cell sorting: Cell sorting was performed on a FACSAria II (BD Biosciences, San Jose, CA) using a 488 nm laser line (chosen for its compatibility with fluorescein isothiocyanate [FITC]) for light scattering and fluorescence excitation. Standard emission filters for FITC and R- phycoerythrin filter were used. To isolate the Cluster of differentiation molecule - 34 and vascular endothelial growth factor receptor -2 positive cells (CD34+/VEGFR2+) cells from other mononuclear precursor cells, the sample was blocked with 10% goat serum (Gibco, Carlsbad, CA) and labeled with the following fluorescent antibodies for 20 min each at 4 °C: anti-VEGFR-2-phycoerythrin (1:200, BD PharMingen, San Jose, CA) and anti-CD34-FITC (1:200, eBioscience, San Diego, CA). Cells were then sorted with flow cytometry (BD Biosciences FACSAria, University of Chicago Flow Cytometry Facility, Chicago, IL) to isolate double positive cells exhibiting both cell surface markers.

Cell viability: HRMEC viability was determined using the CellTiter-Glo Luminescent cell viability assay kit (Promega, Madison, WI). The reagent determines the number of viable cells in culture by quantifying cellular ATP. The HRMECs were added to 96-well plates at a density of 20,000 cells/well in 150 µl of MCDB 131 complete media. The cells were reverse transfected with *FAM18B* siRNA or negative control siRNA at a final concentration of 50 nM using the Lipofectamine RNAiMAX Transfection Reagent for 72 h. Following transfection, the cells were treated with media alone or media containing 50 ng/ml VEGF or 30 mM glucose. To determine the role of NF-κB, cells were pretreated for 1 h with 50 µM pyrrolidine dithiocarbamate (PDTC, Sigma), a specific NF-κB inhibitor and for the remaining duration of the treatment. Following 48 h, the media was replaced with 100 µl of PBS and 100 µl of CellTiter-Glo reagent. The plates were placed on an orbital shaker for 2 min and then followed by 10 min at room temperature to stabilize the luminescent signal. The luminescence was measured to determine the ATP levels (Tecan Genios Pro, Tecan US, Morrisville, NC).

Cell migration assay: Cell migration was performed using a modified Boyden chamber method, as described previously [17]. HTS FluoroBlok 24-well cell culture inserts with 8 µm pore size (BD, Franklin Lakes, NJ) coated with gelatin-based coating solution on the lower surface were placed in companion 24-well tissue culture plates (Corning Inc., Corning, NY). *FAM18B* and control siRNA-transfected HRMECs were seeded in the upper chamber at a density of 50,000 cells/well in media alone. The lower chambers contained media alone as control, 50 ng/ml VEGF or 30 mM glucose as treatments. To determine the role of NF-κB, cells were pretreated for 1 h with 50 µM PDTC (Sigma), a specific NF-κB inhibitor, and for the remaining duration of the treatment. After 18 h of incubation at 37 °C, the culture inserts were removed and placed in 24-well plates containing 2 µM Calcein AM (BD Biosciences, Bedford, MA) in PBS. The cells were further at incubated 37 °C in calcein AM containing PBS for 1 h. Following incubation, the fluorescence in plates was measured with a spectroflurometer at excitation and emission wavelengths of 488 nm and 520 nm (Tecan Genios Pro).

Tube formation assay: A tube formation assay was performed as described previously [17]. Each well of the 96-well tissue culture plates (Costar; Corning) was coated with 50 µl of growth factor-reduced basement membrane matrix (BD Matrigel; BD Biosciences) [17]. FAM18B and control siRNA-transfected HRMECs were added to each well at a density of 20,000/100 µl/well. Serum-free and growth factor-free MCDB 131 media alone or media containing 50 ng/ml VEGF were added to the appropriate wells, and the cells were incubated at 37 °C for 6 h. To determine the role of NF-κB, the cells were pretreated for 1 h with 5,050 µM PDTC (Sigma), a specific NF-κB inhibitor, and for the remaining duration of the treatment. Tube formation was observed under a microscope (Zeiss 710). Images were captured, and the tube length was measured using ImageJ.

Statistical analyses: Data are presented as mean±standard deviation (SD) with statistical differences between groups analyzed with a standard two-tailed Student *t* test using

Microsoft Excel software. A p value of less than 0.05 was considered statistically significant.

RESULTS

FAM18B is expressed in the human retina: We evaluated the presence of *FAM18B* in the retina of human donor eyes. The distribution of *FAM18B* was assessed in the eyes of two normal donors without diabetes (Figure 1). Immunohistochemistry (Figure 1B,C) and immunofluorescence (Figure 1E,F) revealed the presence of *FAM18B* in the human retina (red). *FAM18B* was distinctly colocalized with the retina vasculature. In particular, immunofluorescence demonstrated prominent staining in the retinal vasculature including capillaries, arteriole, and venules. The staining in the vasculature was confined to the endothelium. Staining for *FAM18B* was also observed in the choroidal vasculature. Retinal sections incubated with secondary antibody alone served as the control (Figure 1A,B). The control sections lacked the specific endothelium restricted vascular staining of FAM18B observed in sections incubated with anti-*FAM18B* antibody. All sections demonstrated the nonspecific autofluorescence of the RPE.

FAM18B expression is decreased under diabetic conditions in cultured human retinal microvascular endothelial cells: Given the prominent immunolocalization of *FAM18B* to endothelial cells, HRMECs were treated under various diabetic conditions, including high glucose (25 mM), VEGF (1 ng/ml), or AGEs (25 µg/ml), to determine the effect on *FAM18B*. Expression of *FAM18B* was measured with qRT-PCR and western blot. High glucose, VEGF, and AGE treatment all suppressed *FAM18B* in the HRMECs ($p<0.05$; Figure 2A,B). Control incubation of HRMECs with 25 mM mannose for 24 h, however, did not induce any detectable changes in the *FAM18B* mRNA levels (data not shown), thus underscoring that the observed *FAM18B* suppression was a glucose-specific response.

FAM18B downregulation affects human retinal microvascular endothelial cell viability: To further investigate the mechanistic role of *FAM18B*, HRMECs transfected with control or *FAM18B* siRNA were treated with VEGF (50 ng/ml) or high glucose (30 mM) or media alone with normal glucose (5 mM). Following 48 h of treatment, the cell viability was measured. The cell viability in treatment groups was normalized to HRMECs treated with transfected scrambled control siRNA in media alone. The viability across the treatment groups is expressed as percent viability compared to the control cells (Figure 3A–C). The percent viability of the control siRNA-transfected cells treated with VEGF and high glucose compared to cells treated with medium alone was 130.8±19 and 88±17.7. The percent viability of the *FAM18B* siRNA-transfected cells treated with media alone, VEGF, and high glucose was 91.9±14.4, 117.4±23.8, and 52.4±21.5, respectively. Although the *FAM18B* siRNA-transfected cells demonstrated decreased viability, the difference was not significant. VEGF increased the viability of the control siRNA-transfected HRMECs by 30% ($p<0.05$) while in *FAM18B* siRNA-transfected cells VEGF increased viability by only 17% compared to the control cells. Although there

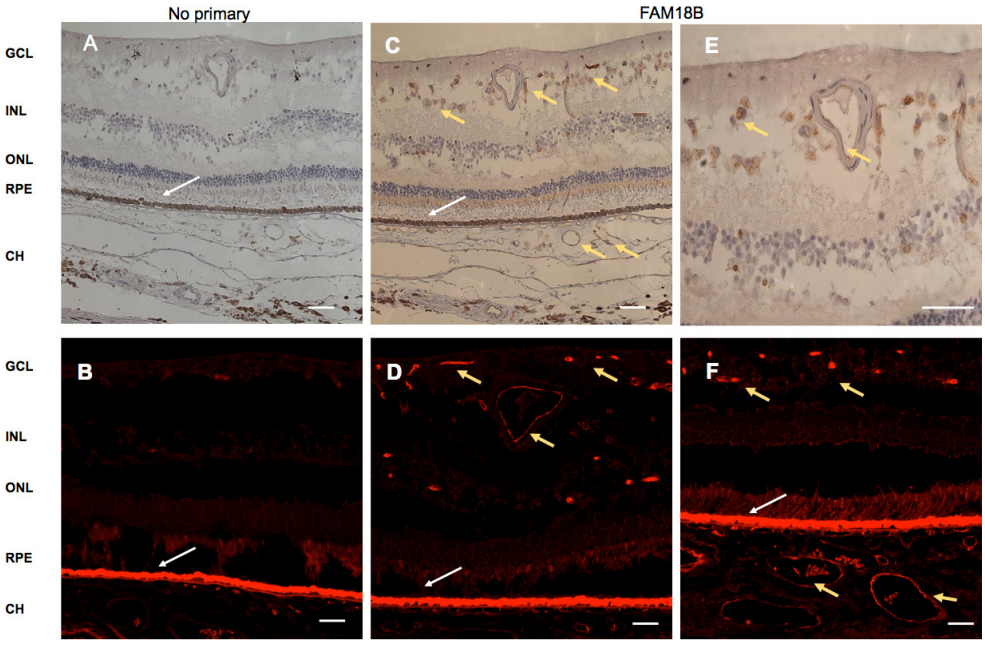

Figure 1. Immunolocalization of *FAM18B* in the human retina. **A**, **B**: Negative controls for immunohistochemistry and immunofluorescence, respectively. Autofluorescence is evident in the RPE (white arrow). Immunohistochemistry demonstrates *FAM18B* (brown) in the retinal and choroidal vasculature (yellow arrows; **C**, **E**). Immunofluorescence reveals a prominent signal for the *FAM18B* (red) in the retinal and choroidal vasculature (yellow arrows; **D**, **F**).

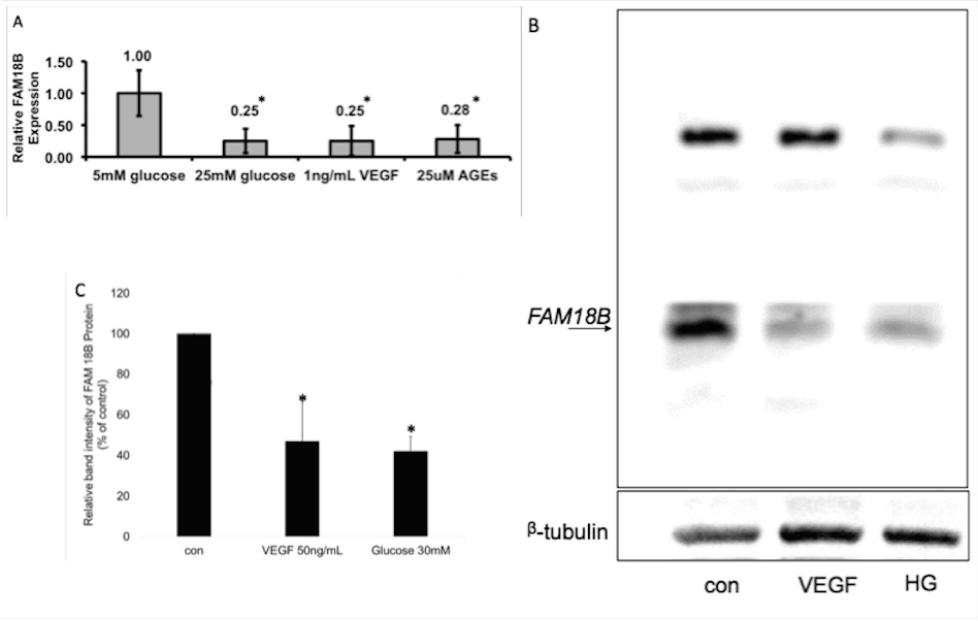

Figure 2. Decreased *FAM18B* expression under diabetic conditions in cultured human retinal microvascular endothelial cells. **A**: There are significant decreases in the *FAM18B* mRNA levels in human retinal microvascular endothelial cells (HRMECs) treated with 25 mM glucose, 1 ng/ml vascular endothelial growth factor (VEGF), and 25 µM advanced glycation end products (AGEs), compared with 5 mM glucose. **B**: Western blot of the FAM18B protein and β-tubulin in HRMECs following treatment with VEGF 50 ng/ml and glucose 30 mM for 48 h reveals decreased protein expression. **C**: Quantification of the FAM18B protein band intensities normalized to β-tubulin band intensities in HRMECs following treatment with VEGF 50 ng/ml and glucose 30 mM for 48 h. Data are represented as percent change mean±standard deviation (SD) regarding control cells treated with media alone (n=3). * p value <0.05 compared to control.

was a decrease in the viability of control siRNA-transfected cells with high glucose, this was not significant. Cells transfected with *FAM18B* siRNA exhibited a significant reduction in viability by 50% when exposed to high glucose ($p<0.05$). The high glucose–induced decrease in viability in the *FAM18B*-depleted cells was significantly reversed by PDTC, a specific NF-κB inhibitor ($p<0.05$). These data suggest that the presence of *FAM18B* may help protect retinal endothelial cells from glucose-induced damage.

FAM18B downregulation affects human retinal microvascular endothelial cell migration: Migration of HRMECs was determined using a modified Boyden chamber assay. Migration of HRMECs transfected with scrambled control siRNA and treated with media alone served as the control. Migration across treatment groups was expressed as percent migration compared to control (Figure 4A–C). The percent migration of HRMECs transfected with control siRNA and treated with media alone, high glucose, VEGF, or PDTC was 100.41±4.78, 127.79±0.01, 179.04±8.02, and 81.84±6.19, respectively. The percent migration of *FAM18B* siRNA-transfected cells treated with media alone, high glucose (30 mM), VEGF (50 ng/ml), or PDTC was 142.07±8.25, 173.50±11.19, 279.01±9.79, and 84.21±15.81, respectively. *FAM18B* siRNA-transfected cells demonstrated a 40% increase in migration compared to scrambled control cells ($p<0.05$). The increase in migration of HRMEC in *FAM18B* siRNA-treated cells was significantly inhibited by PDTC, an NF-κB inhibitor. VEGF and high glucose both significantly increased the migration of control and *FAM18B* siRNA-transfected cells. Moreover, VEGF and high glucose significantly potentiated the migration of *FAM18B* siRNA-transfected cells over control siRNA-transfected cells.

FAM18B downregulation affects human retinal microvascular endothelial cell tube formation: The ability of HRMECs to form tubes in BD Matrigel was determined using the in vitro tube formation assay (Figure 5A–C). HRMECs transfected with scrambled control siRNA and treated with media alone served as control. The percent total tube length of HRMECs transfected with control siRNA and treated with media alone, VEGF, or PDTC was 104.35±5.84, 165.3±25.32, and 44.83±6.06, respectively. The percent total tube length of *FAM18B* siRNA-transfected cells treated with media alone and VEGF was 213.48±20.72, 225.10±5.23, and 104.54±8.88, respectively. *FAM18B* siRNA-transfected cells demonstrated a significant twofold increased tube formation compared to the scrambled control cells ($p<0.05$). The increase in endothelial tube formation following *FAM18B* depletion was markedly inhibited by PDTC, a specific NF-κB inhibitor. VEGF significantly increased tube formation in control cells; however, VEGF had no effect on tube formation in *FAM18B* siRNA-transfected cells.

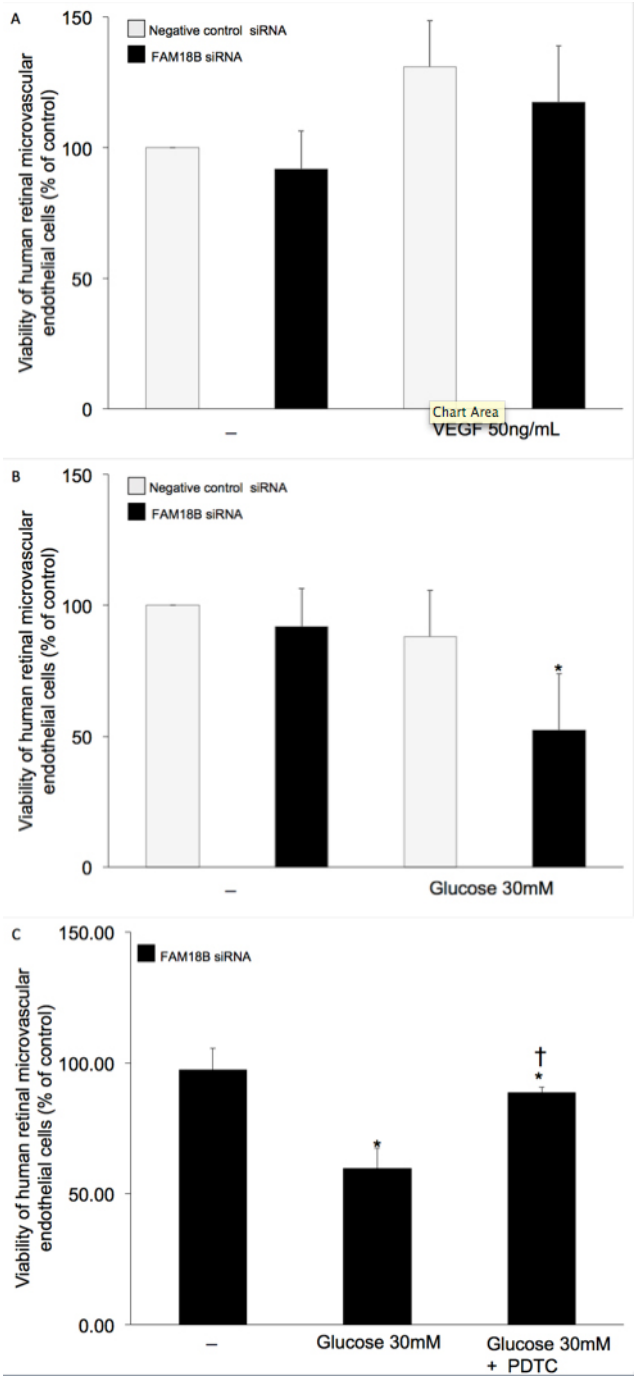

Figure 3. Effect of *FAM18B* knockdown on human retinal microvascular endothelial cell viability. The viability of human retinal microvascular endothelial cells (HRMECs) in various treatment groups are expressed as the percent viability of HRMECs transfected with scrambled control siRNA and treated with medium alone unless specified otherwise. **A**: Viability of HRMECs transfected with scrambled control siRNA or *FAM18B* siRNA treated with or without vascular endothelial growth factor (VEGF). **B**: Viability of HRMECs transfected with scrambled control siRNA or *FAM18B* siRNA treated with or without high glucose. **C**: Viability of HRMECs transfected with *FAM18B* siRNA treated with high glucose in the presence or absence pyrrolidine dithiocarbamate (PDTC). **A**–**C**: PDTC is a specific nuclear factor-kappa B (NF-κB) inhibitor. Data represented as mean±standard deviation (SD) (n=3×96-well plates; four wells/plate for panels **B** and **C** and n=1×96 well plate; five wells/plate for panel **A**). * p value <0.05 compared to control cells treated with media alone. †p value <0.05 compared to *FAM18B* siRNA-transfected cells treated with high glucose.

FAM18B expression is decreased in CD34+/VEGFR2+ cells: Eye tissue from post-mortem specimens may have altered gene expression profiles depending on the time of acquisition and the nature of storage [18]. Cells from the peripheral blood, such as CD34+/VEGFR2+ mononuclear cells, are easily accessible and can be obtained quickly and noninvasively. We sought to examine these circulating cells in subjects with proliferative diabetic retinopathy to confirm our in vitro *FAM18B* findings (Figure 6). Previous studies exploring pathologic retinal angiogenesis suggest this population of mononuclear cells may contribute to pathologic retinal neovascularization thus making them a clinically relevant accessible peripheral population of cells in human patients [19-27].

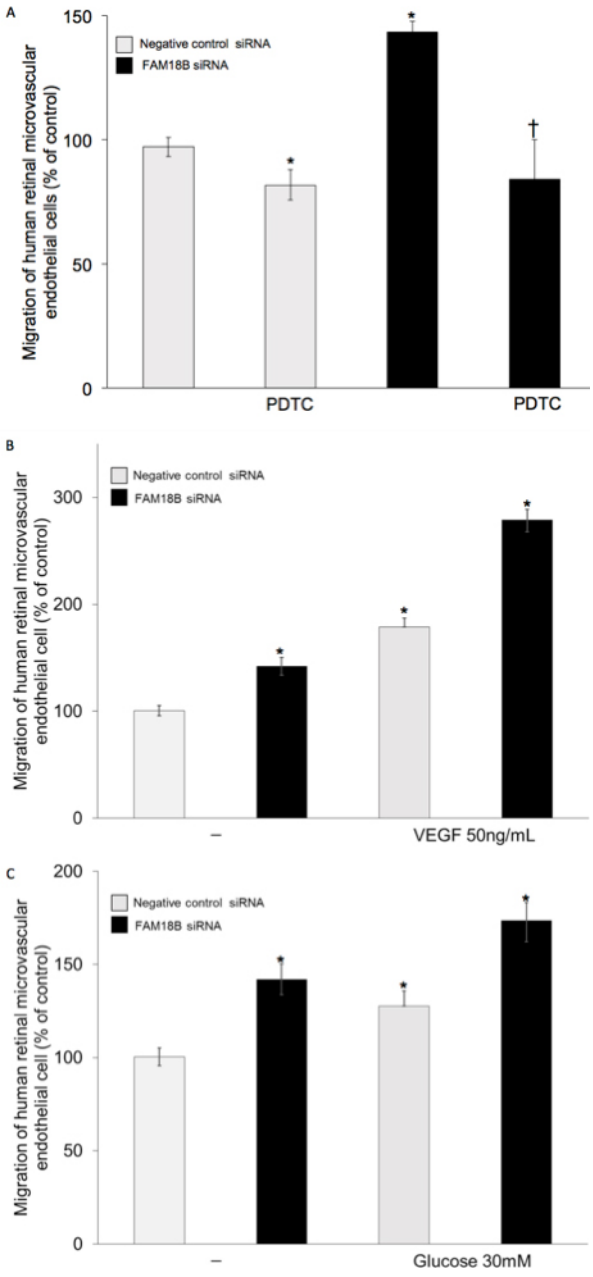

Figure 4. Effect of *FAM18B* knockdown on human retinal microvascular endothelial cell migration. The migration of human retinal microvascular endothelial cells (HRMECs) in various treatment groups are expressed as percent change of HRMECs transfected with scrambled control siRNA and treated with medium alone. **A**: Migration of HRMECs transfected with scrambled control siRNA or *FAM18B* siRNA in the presence or absence of pyrrolidine dithiocarbamate (PDTC). *FAM18B* knockdown significantly increases the basal migration of HRMECs. **B**: Migration of HRMECs transfected with scrambled control siRNA or *FAM18B* siRNA treated with or without vascular endothelial growth factor (VEGF). **C**: Migration of HRMECs transfected with scrambled control siRNA or *FAM18B* siRNA treated with or without high glucose. PDTC is a specific nuclear factor-kappa B (NF-κB) inhibitor. VEGF and glucose significantly increase the migration of control cells. The VEGF and glucose-induced migration is further potentiated in *FAM18B* siRNA-transfected cells. The data are represented as mean±standard deviation (SD) * p-value <0.05 compared to control cells treated with media alone. † p value <0.05 compared to *FAM18B* siRNA-transfected cells.

There were no substantive differences between the study groups at baseline (Table 1). The mean age (± SD) of subjects in the control group was 56.8 (± 14.6) while the mean age (± SD) of the subjects in the experimental group was 59.1 (± 12.4), yielding no significant age differences between groups (p=0.73). Gender (p=0.26) and ethnicity (p=0.62) similarly were not significant between the groups, with most subjects from both groups identifying as African American. Last, there was no significant difference between the groups in the duration of diagnosis of diabetes (p=0.22) or recorded blood glucose level at last visit (p=0.06). The average diabetes duration (± SD) for the control subjects was 9.9 (± 6.5) years, and the mean time since diagnosis (± SD) for the study subjects was 18.3 (± 12.6) years. The average blood glucose level (BSL; ± SD) for the controls was 143.4 (± 36.7) mg/dl, and the average BSL (± SD) for the proliferative diabetic retinopathy subjects was 195.6 (± 54.6) mg/dl. Although these differences were not significant, there was a general trend toward increasing diabetes duration and increasing basal sugar level in the proliferative diabetic retinopathy subjects. HbA_1c levels were not used to determine glycemic control because they were not uniformly recorded for all subjects,

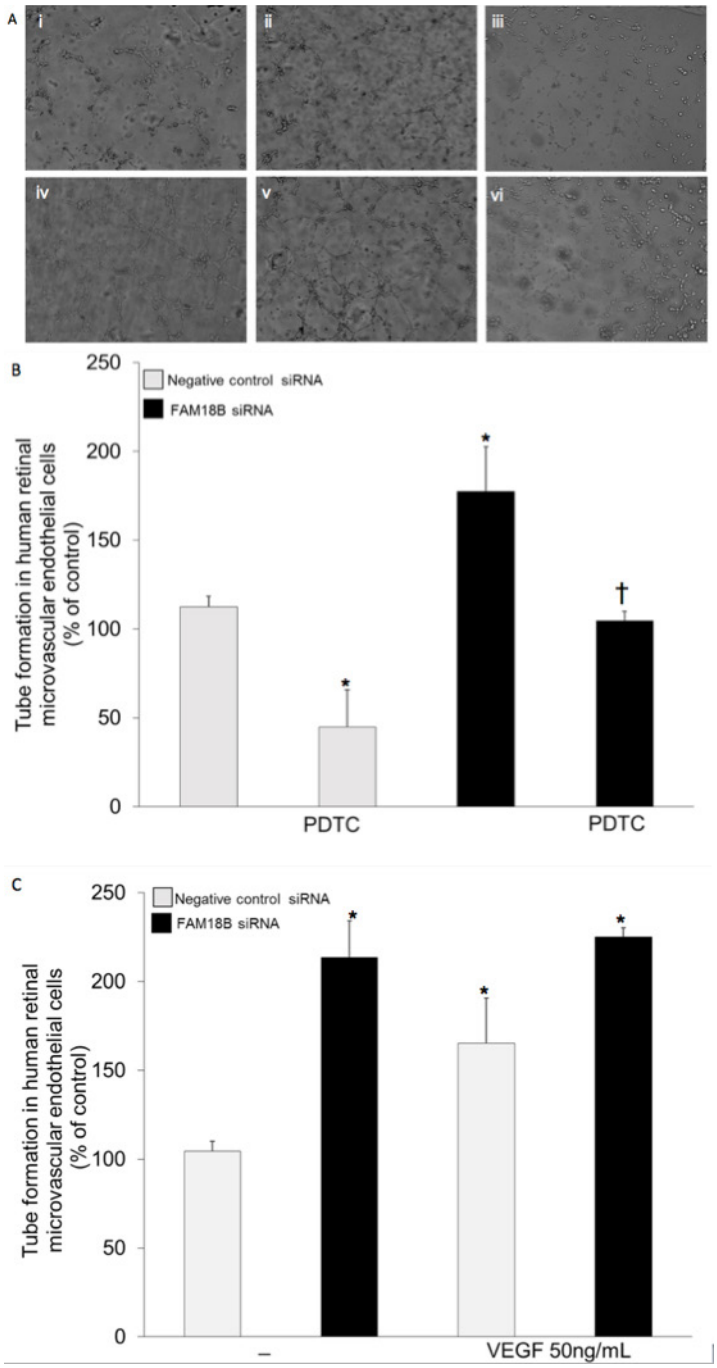

Figure 5. Effect of *FAM18B* knockdown on human retinal microvascular endothelial cell tube formation. **A**: Representative images of tube formation in various treatment groups. (i) Scrambled control; (ii) scrambled control treated with vascular endothelial growth factor (VEGF); and (iii) scrambled control treated with pyrrolidine dithiocarbamate (PDTC). (iv) *FAM18B* siRNA-treated cells; (v) *FAM18B* siRNA treated with VEGF; and (vi) *FAM18B* siRNA treated with PDTC. **B**: The tube formation of human retinal microvascular endothelial cells (HRMECs) in transfected with scrambled control siRNA or *FAM18B* transfected siRNA treated with or without PDTC. *FAM18B* knockdown increases the basal tube formation of HRMECs. The enhanced basal tube formation is inhibited by PDTC, a specific nuclear factor-kappa B (NF-κB) inhibitor. **C**: Tube formation in control siRNA-transfected cells and *FAM18B* siRNA-transfected cells treated with or without VEGF. VEGF increases tube formation of control cells but not in *FAM18B* siRNA transfected cells. The data are represented as mean±standard deviation (SD) (n=3). * p value <0.05 compared to control cells treated with media alone. † p value <0.05 compared to *FAM18B* siRNA-transfected cells.

and therefore, the BSL was the most consistent information available from a chart review regarding glycemic control.

CD34+/VEGFR2+ cells were isolated using flow cytometry (Figure 7). Relative mRNA expression levels of *FAM18B* were compared in CD34+/VEGFR2+ cells from diabetic subjects with or without proliferative diabetic retinopathy. GAPDH mRNA was used as the internal standard for normalization. The expression levels as determined by the $2^{-\Delta\Delta c}{}_{t}$ values of *FAM18B* in diabetic patients with no retinopathy were 1.03±0.12, and the levels in diabetic patients with proliferative diabetic retinopathy were 0.81±0.11. The *FAM18B* expression levels were significantly decreased in the patients with proliferative diabetic retinopathy compared with the diabetes group without retinopathy (Figure 8; $p<0.05$).

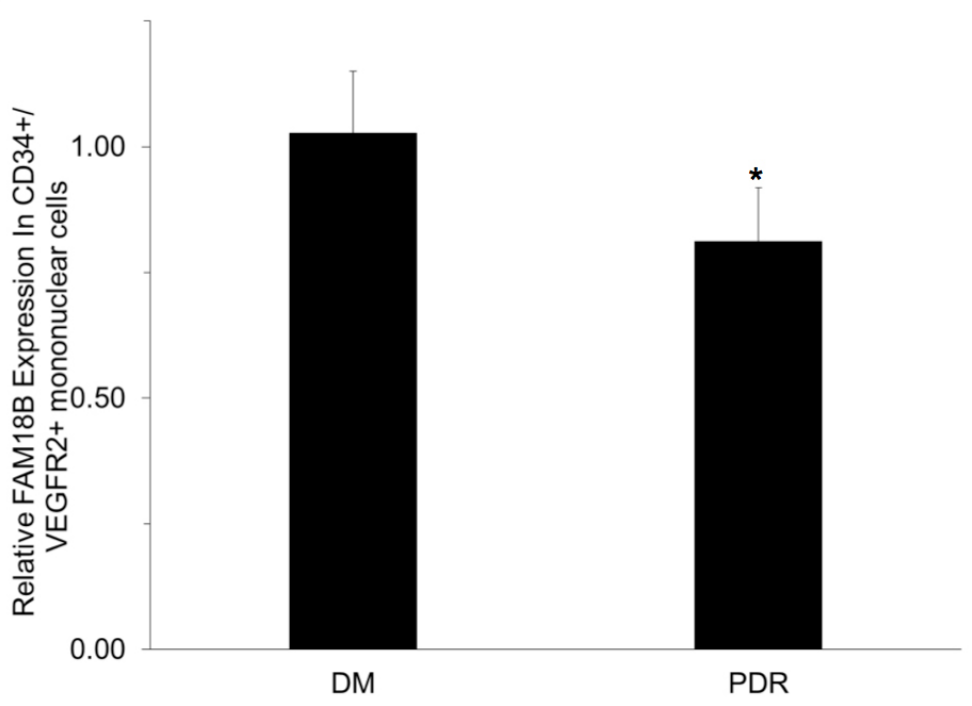

Figure 6. Decreased *FAM18B* expression in CD34+/VEGFR2+ cells. Expression of *FAM18B* in CD34+/VEGFR2+ mononuclear cells from diabetic subjects with proliferative diabetic retinopathy is decreased compared to diabetic subjects without retinopathy. Glyceraldehyde 3-phosphate dehydrogenase (GAPDH) mRNA was used as internal standard for normalization. DM: diabetes without diabetic retinopathy (n=9). PDR: diabetes with proliferative diabetic retinopathy (n=8). *p-value <0.05.

DISCUSSION

For the study of diabetic retinopathy, candidate gene studies were initially performed to evaluate genes in the major mechanistic pathways thought to be important in the development of microvascular complications associated with diabetes. To date, these studies have enjoyed limited success [28-32]. Strong evidence exists that there is a significant genetic component to diabetic retinopathy severity, yet to date, few genes or pathways have reliably been associated with the development of this disorder. We used a genome-wide association approach to agnostically implicate those critical genes and biologic pathways dysregulated in this condition [14]. *FAM18B* encodes for a membrane protein with unknown function. The gene was investigated in this study based on the association of a *FAM18B* intronic SNP, rs11871508, with diabetic retinopathy in our recent GWAS [14].

Diabetic retinopathy significantly affects the normal functioning of retinal vasculature. Various mediators including hyperglycemia, AGEs, cytokines, and reactive oxygen species have been implicated in retinal microvascular injury. Associated ischemia and secondary hypoxia further drive the upregulation of angiogenic factors including VEGF that can result in angiogenesis and pathologic neovascularization seen in proliferative diabetic retinopathy.

Immunohistochemistry and immunofluorescence findings from this study demonstrate that *FAM18B* is expressed in the retina. Given the prominent endothelial immunolocalization, we investigated *FAM18B* expression in HRMECs. We observed that *FAM18B* expression was decreased in HRMECs exposed to various in vitro diabetic conditions, including high glucose, VEGF, or AGEs. To determine the functional role of *FAM18B* in HRMECs, we experimentally knocked down the levels of *FAM18B* with siRNA. Interestingly, we observed that the RNAi-mediated knockdown of *FAM18B* in HRMECs increased migration and endothelial tube formation. Importantly, we observed that VEGF or high glucose–induced migration was significantly potentiated in *FAM18B*-depleted HRMECs. We also observed that in the *FAM18B*-depleted cells, high glucose markedly exacerbated endothelial cell viability.

NF-κB is known to be upregulated in the setting of diabetes and plays a key role in its microvascular complications [33-36]. A transcription factor with multiple functions, NF-κB has been implicated in mediating hyperglycemia-induced retinal endothelial cell death through apoptosis in diabetes and regulating VEGF levels and VEGF-induced angiogenesis in diabetic retinopathy [37]. VEGF, in turn, can activate proinflammatory NF-κB signaling and downstream effects such as the enhanced expression of adhesion molecules in endothelial cells and the secretion of inflammatory cytokines [8,9]. We therefore explored the effects of NF-κB on the *FAM18B*-depleted endothelial cells using a specific NF-κB inhibitor, PDTC [38-40]. In our studies, we observed

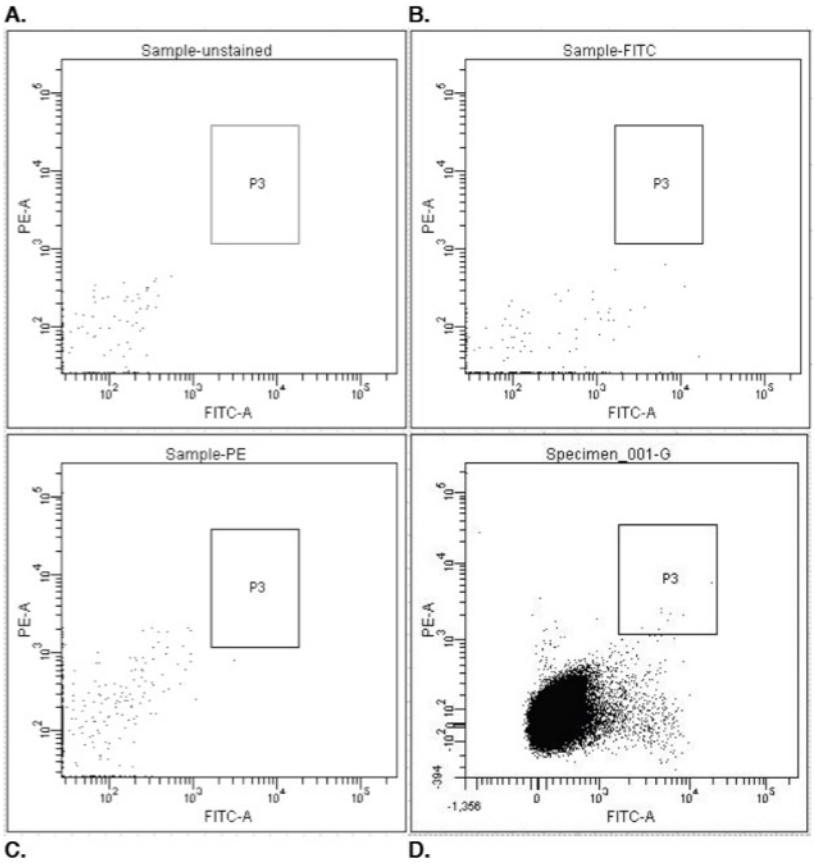

Figure 7. Isolation of CD34+/VEGFR2+ mononuclear cells. Single positive controls and an unstained control were used to set the appropriate compensation values necessary to assign the double positive gating strategy (**A**, **B**, and **C**). Whole cells were separated from debris and doublets using the area and width pulses for forward and side scatter (**D**). The box identifies all double-positive cells that exhibit sufficient fluorescence of both markers to be identified—these were the cells that were sorted and collected.

that NF-κB inhibition reversed the endothelial effects of *FAM18B*-mediated knockdown.

To better interpret these findings within the clinical context of diabetic retinopathy, we evaluated the expression of *FAM18B* in CD34+/VEGFR2+ mononuclear cells from individuals with proliferative diabetic retinopathy. Cells from the peripheral blood, such as CD34+/VEGFR2+ cells, are considered one of the circulating populations that may play a role in the normal physiology of the retinal capillary bed as well as its dysregulation in proliferative retinopathy [22,24,26]. CD34+/VEGFR2+ mononuclear cells in diabetic subjects demonstrate impaired proliferation and incorporation in vasculature thus limiting the normal repair of vasculature [41]. In advanced stages of proliferative diabetic retinopathy, these cells have been implicated in pathogenic neovascularization [42]. Interestingly, we observed the decreased expression of *FAM18B* in circulating CD34+/VEGFR2+ mononuclear cells obtained from subjects with proliferative diabetic retinopathy when compared to subjects with no diabetic retinopathy. Although *FAM18B* levels in CD34+/VEGFR2+ mononuclear may not necessarily reflect its levels in the retinal endothelium, the low levels of *FAM18B* in the circulating cells in patients with proliferative retinopathy are consistent with our in vitro findings.

In summary, this is the first study to show the expression of the FAM18B protein in the human retina. We further have demonstrated that the expression of *FAM18B* is significantly decreased in human retinal microvascular endothelial cells when exposed to diabetic stimuli including high glucose and VEGF. Further, we demonstrated that RNAi-mediated downregulation of *FAM18B* enhances migration as well as endothelial tube formation in HRMECs and potentiates high glucose–induced endothelial cell death. Finally, we show that subjects with proliferative diabetic retinopathy exhibit reduced *FAM18B* expression. Thus, this study suggests a potential role for *FAM18B* in diabetic retinopathy.

ACKNOWLEDGMENTS

The authors gratefully acknowledge support from the following organizations for this research: NIH K08EY019089-02, Diabetes Research and Training Center P60DK020595-32, Illinois Society for the Prevention of Blindness, Fight for Sight, OneSight, Knight's Templar Eye Foundation, the Louis Block fund, and the International Retinal Research

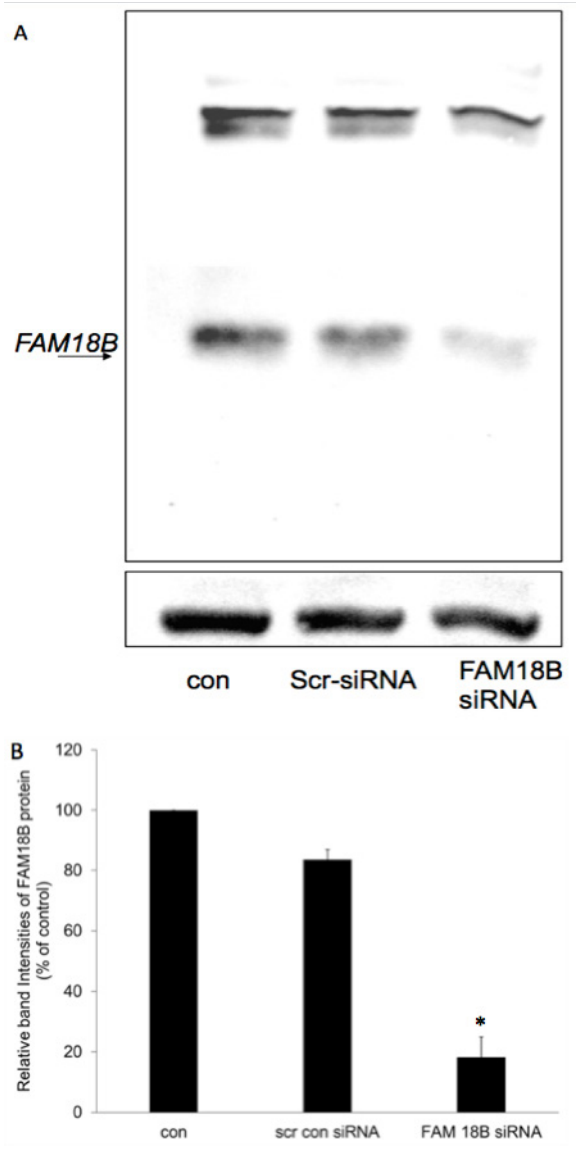

Figure 8. RNAi-mediated downregulation of *FAM18B* in human retinal microvascular endothelial cells. **A**: Representative western blot of the FAM18B protein and β-tubulin in human retinal microvascular endothelial cells (HRMECs) following transfection with control siRNA and *FAM18B* siRNA for 72 h. **B**: Quantification of the FAM18B protein band intensities normalized to β-tubulin band intensities in HRMECs. Data are represented as percent change. Mean±standard deviation (SD) regarding cells treated with media alone (n=2). * p value <0.05.

Foundation. This study was also supported by the National Eye Institute Core Grant P30EY001792 for Vision Research and an unrestricted grant from Research to Prevent Blindness, Inc., New York, NY. The content is solely the responsibility of the authors and does not necessarily represent the official views of the NIH. The authors are appreciative to Dr. G. Bell and Dr. D. Nicolae (Unniversity of Chicago, IL) for many helpful discussions. The authors thank R. Zelka (University of Illinois at Chicago) for her help with imaging and microscopy.

REFERENCES

1. National diabetes fact sheet: national estimates and general information on diabetes and prediabetes in the United States. 2011 [cited 2012 02/02/2012]; Available from: http://www.cdc.gov/diabetes/pubs/pdf/ndfs_2011.pdf
2. Tarr JM, Kaul K, Chopra M, Kohner EM, Chibber R. Pathophysiology of Diabetic Retinopathy. ISRN 2013; 2013:343560-[PMID: 24563789].
3. Klein R. Hyperglycemia and microvascular and macrovascular disease in diabetes. Diabetes Care 1995; 18:258-68. [PMID: 7729308].
4. Engerman RL, Kern TS. Hyperglycemia as a cause of diabetic retinopathy. Metabolism 1986; 35:Suppl 120-3. [PMID: 3083205].

5. Caldwell RB, Bartoli M, Behzadian MA, El-Remessy AE, Al-Shabrawey M, Platt DH, Caldwell RW. Vascular endothelial growth factor and diabetic retinopathy: pathophysiological mechanisms and treatment perspectives. Diabetes Metab Res Rev 2003; 19:442-55. [PMID: 14648803].

6. Caldwell RB, Bartoli M, Behzadian MA, El-Remessy AE, Al-Shabrawey M, Platt DH, Liou GI, Caldwell RW. Vascular endothelial growth factor and diabetic retinopathy: role of oxidative stress. Curr Drug Targets 2005; 6:511-24. [PMID: 16026270].

7. Crawford TN, Alfaro DV 3rd, Kerrison JB, Jablon EP. Diabetic retinopathy and angiogenesis. Curr Diabetes Rev 2009; 5:8-13. [PMID: 19199892].

8. Kim I, Moon SO, Kim SH, Kim HJ, Koh YS, Koh GY. Vascular endothelial growth factor expression of intercellular adhesion molecule 1 (ICAM-1), vascular cell adhesion molecule 1 (VCAM-1), and E-selectin through nuclear factor-kappa B activation in endothelial cells. J Biol Chem 2001; 276:7614-20. [PMID: 11108718].

9. Marumo T, Schini-Kerth VB, Busse R. Vascular endothelial growth factor activates nuclear factor-kappaB and induces monocyte chemoattractant protein-1 in bovine retinal endothelial cells. Diabetes 1999; 48:1131-7. [PMID: 10331420].

10. Madsen-Bouterse SA, Kowluru RA. Oxidative stress and diabetic retinopathy: pathophysiological mechanisms and treatment perspectives. Rev Endocr Metab Disord 2008; 9:315-27. [PMID: 18654858].

11. King GL, Loeken MR. Hyperglycemia-induced oxidative stress in diabetic complications. Histochem Cell Biol 2004; 122:333-8. [PMID: 15257460].

12. Intensive blood-glucose control with sulphonylureas or insulin compared with conventional treatment and risk of complications in patients with type 2 diabetes (UKPDS 33). UK Prospective Diabetes Study (UKPDS) Group. Lancet 1998; 352:837-53. [PMID: 9742976].

13. Clustering of long-term complications in families with diabetes in the diabetes control and complications trial. The Diabetes Control and Complications Trial Research Group. Diabetes 1997; 46:1829-39. [PMID: 9356033].

14. Grassi MA, Tikhomirov A, Ramalingam S, Below JE, Cox NJ, Nicolae DL. Genome-wide meta-analysis for severe diabetic retinopathy. Hum Mol Genet 2011; 20:2472-81. [PMID: 21441570].

15. Grassi MA, Tikhomirov A, Ramalingam S, Lee KE, Hosseini SM, Klein BE, Klein R, Lussier YA, Cox NJ, Nicolae DL. Replication analysis for severe diabetic retinopathy. Invest Ophthalmol Vis Sci 2012; 53:2377-81. [PMID: 22427569].

16. Lai CH, Chou CY, Ch'ang LY, Liu CS, Lin W. Identification of novel human genes evolutionarily conserved in Caenorhabditis elegans by comparative proteomics. Genome Res 2000; 10:703-13. [PMID: 10810093].

17. Bajpai AK, Blaskova E, Pakala SB, Zhao T, Glasgow WC, Penn JS, Johnson DA, Rao GN. 15(S)-HETE production in human retinal microvascular endothelial cells by hypoxia: Novel role for MEK1 in 15(S)-HETE induced angiogenesis. Invest Ophthalmol Vis Sci 2007; 48:4930-8. [PMID: 17962441].

18. Hallman DM, Huber JC Jr, Gonzalez VH, Klein BE, Klein R, Hanis CL. Familial aggregation of severity of diabetic retinopathy in Mexican Americans from Starr County, Texas. Diabetes Care 2005; 28:1163-8. [PMID: 15855583].

19. Brunner S, Schernthaner GH, Satler M, Elhenicky M, Hoellerl F, Schmid-Kubista KE, Zeiler F, Binder S, Schernthaner G. Correlation of different circulating endothelial progenitor cells to stages of diabetic retinopathy: first in vivo data. Invest Ophthalmol Vis Sci 2009; 50:392-8. [PMID: 18719083].

20. Peichev M, Naiyer AJ, Pereira D, Zhu Z, Lane WJ, Williams M, Oz MC, Hicklin DJ, Witte L, Moore MA, Rafii S. Expression of VEGFR-2 and AC133 by circulating human CD34(+) cells identifies a population of functional endothelial precursors. Blood 2000; 95:952-8. [PMID: 10648408].

21. Gehling UM, Ergun S, Schumacher U, Wagener C, Pantel K, Otte M, Schuch G, Schafhausen P, Mende T, Kilic N, Kluge K, Schafer B, Hossfeld DK, Fiedler W. In vitro differentiation of endothelial cells from AC133-positive progenitor cells. Blood 2000; 95:3106-12. [PMID: 10807776].

22. Asnaghi V, Lattanzio R, Mazzolari G, Pastore MR, Ramoni A, Maestroni A, Ruggieri D, Luzi L, Brancato R, Zerbini G. Increased clonogenic potential of circulating endothelial progenitor cells in patients with type 1 diabetes and proliferative retinopathy. Diabetologia 2006; 49:1109-11. [PMID: 16520918].

23. Yoder MC. Is endothelium the origin of endothelial progenitor cells? Arterioscler Thromb Vasc Biol 2010; 30:1094-103. [PMID: 20453169].

24. Caballero S, Sengupta N, Afzal A, Chang KH, Li Calzi S, Guberski DL, Kern TS, Grant MB. Ischemic vascular damage can be repaired by healthy, but not diabetic, endothelial progenitor cells. Diabetes 2007; 56:960-7. [PMID: 17395742].

25. Asahara T, Murohara T, Sullivan A, Silver M, van der Zee R, Li T, Witzenbichler B, Schatteman G, Isner JM. Isolation of putative progenitor endothelial cells for angiogenesis. Science 1997; 275:964-7. [PMID: 9020076].

26. Butler JM, Guthrie SM, Koc M, Afzal A, Caballero S, Brooks HL, Mames RN, Segal MS, Grant MB, Scott EW. SDF-1 is both necessary and sufficient to promote proliferative retinopathy. J Clin Invest 2005; 115:86-93. [PMID: 15630447].

27. Sieveking DP, Buckle A, Celermajer DS, Ng MK. Strikingly different angiogenic properties of endothelial progenitor cell subpopulations: insights from a novel human angiogenesis assay. J Am Coll Cardiol 2008; 51:660-8. [PMID: 18261686].

28. Ko BC, Lam KS, Wat NM, Chung SS. An (A-C)n dinucleotide repeat polymorphic marker at the 5′ end of the aldose reductase gene is associated with early-onset diabetic retinopathy in NIDDM patients. Diabetes 1995; 44:727-32. [PMID: 7789640].

29. Warpeha KM, Chakravarthy U. Molecular genetics of microvascular disease in diabetic retinopathy. Eye (Lond) 2003; 17:305-11. [PMID: 12724690].

30. Al-Kateb H, Mirea L, Xie X, Sun L, Liu M, Chen H, Bull SB, Boright AP, Paterson AD. Multiple variants in vascular endothelial growth factor (VEGFA) are risk factors for time to severe retinopathy in type 1 diabetes: the DCCT/EDIC genetics study. Diabetes 2007; 56:2161-8. [PMID: 17513698].

31. Luo J, Zhao L, Chen AY, Zhang X, Zhu J, Zhao J, Ouyang H, Luo H, Song Y, Lee J, Patel SH, Shaw PX, Sadda S, Zhuo Y, Rosenfeld MG, Zhang K. TCF7L2 variation and proliferative diabetic retinopathy. Diabetes 2013; 62:2613-7. [PMID: 23434931].

32. Tong Z, Yang Z, Patel S, Chen H, Gibbs D, Yang X, Hau VS, Kaminoh Y, Harmon J, Pearson E, Buehler J, Chen Y, Yu B, Tinkham NH, Zabriskie NA, Zeng J, Luo L, Sun JK, Prakash M, Hamam RN, Tonna S, Constantine R, Ronquillo CC, Sadda S, Avery RL, Brand JM, London N, Anduze AL, King GL, Bernstein PS, Watkins S. Genetics of D, Diabetic Complication Study G, Jorde LB, Li DY, Aiello LP, Pollak MR, Zhang K. Promoter polymorphism of the erythropoietin gene in severe diabetic eye and kidney complications. Proc Natl Acad Sci USA 2008; 105:6998-7003. [PMID: 18458324].

33. Kowluru RA, Koppolu P, Chakrabarti S, Chen S. Diabetes-induced activation of nuclear transcriptional factor in the retina, and its inhibition by antioxidants. Free Radic Res 2003; 37:1169-80. [PMID: 14703729].

34. Morigi M, Angioletti S, Imberti B, Donadelli R, Micheletti G, Figliuzzi M, Remuzzi A, Zoja C, Remuzzi G. Leukocyte-endothelial interaction is augmented by high glucose concentrations and hyperglycemia in a NF-kB-dependent fashion. J Clin Invest 1998; 101:1905-15. [PMID: 9576755].

35. Hofmann MA, Schiekofer S, Kanitz M, Klevesath MS, Joswig M, Lee V, Morcos M, Tritschler H, Ziegler R, Wahl P, Bierhaus A, Nawroth PP. Insufficient glycemic control increases nuclear factor-kappa B binding activity in peripheral blood mononuclear cells isolated from patients with type 1 diabetes. Diabetes Care 1998; 21:1310-6. [PMID: 9702439].

36. Hofmann MA, Schiekofer S, Isermann B, Kanitz M, Henkels M, Joswig M, Treusch A, Morcos M, Weiss T, Borcea V, Abdel Khalek AK, Amiral J, Tritschler H, Ritz E, Wahl P, Ziegler R, Bierhaus A, Nawroth PP. Peripheral blood mononuclear cells isolated from patients with diabetic nephropathy show increased activation of the oxidative-stress sensitive transcription factor NF-kappaB. Diabetologia 1999; 42:222-32. [PMID: 10064103].

37. Kowluru RA, Koppolu P, Chakrabarti S, Chen S. Diabetes-induced activation of nuclear transcriptional factor in the retina, and its inhibition by antioxidants. Free Radic Res 2003; 37:1169-80. [PMID: 14703729].

38. Liu SF, Ye X, Malik AB. Inhibition of NF-kappaB activation by pyrrolidine dithiocarbamate prevents In vivo expression of proinflammatory genes. Circulation 1999; 100:1330-7. [PMID: 10491379].

39. Bessho R, Matsubara K, Kubota M, Hirota H, Wakazona Y, Lin W, Okuda A, Kawai M, Nishikomori R. Pyrrolidine dithiocarbamate, a potent inhibitor of nuclear factor kappa B (NF-kappa B) activation, prevents apoptosis in human promyelocytic leukemia HL-60 cells and thymocytes. Biochem Pharmacol 1994; 48:1883-9. [PMID: 7986199].

40. Ho FM, Lin WW, Chen BC, Chao CM, Yang CR, Lin LY, Lai CC, Liu SH, Liau CS. High glucose-induced apoptosis in human vascular endothelial cells is mediated through NF-kappaB and c-Jun NH2-terminal kinase pathway and prevented by PI3K/Akt/eNOS pathway. Cell Signal 2006; 18:391-9. [PMID: 15970429].

41. Tepper OM, Galiano RD, Capla JM, Kalka C, Gagne PJ, Jacobowitz GR, Levine JP, Gurtner GC. Human endothelial progenitor cells from type II diabetics exhibit impaired proliferation, adhesion, and incorporation into vascular structures. Circulation 2002; 106:2781-6. [PMID: 12451003].

42. Lee IG, Chae SL, Kim JC. Involvement of circulating endothelial progenitor cells and vasculogenic factors in the pathogenesis of diabetic retinopathy. Eye (Lond) 2006; 20:546-52. [PMID: 15905870].

Articles are provided courtesy of Emory University and the Zhongshan Ophthalmic Center, Sun Yat-sen University, P.R. China. The print version of this article was created on 4 August 2014. This reflects all typographical corrections and errata to the article through that date. Details of any changes may be found in the online version of the article.